Available online at www.sciencedirect.com

ScienceDirect

materialstoday: PROCEEDINGS

Materials Today: Proceedings 3 (2016) 825 – 831

12th International Conference on Nanosciences & Nanotechnologies & 8th International Symposium on Flexible Organic Electronics

Electron microscopy study on the Influence of B-implantation on Ni induced lateral crystallization in amorphous Si.*

Vouroutzis N.[a]*, Radnóczi G. Z.[b], Dodony E[b], Battistig G.[b], Stoemenos J.[a], Pécz B.[b] and Frangis N.[a]

[a] *Department of Physics, Aristotle University of Thessaloniki, GR-54124 Thessaloniki, Greece*
[b] *Institute for Technical Physics and Matl. Sci., Centre for Energy Research, Hungarian Academy of Sciences, MTA EK MFA,1121 Budapest, Konkoly-Thege u. 29-33*

Abstract

Nickel Metal Induced Lateral Crystallization (Ni-MILC) emerged as a viable technique for crystallization of a-Si films decreasing the crystallization temperature. Boron (B) implantation on a-Si films significantly enhances the crystallization rate of the Ni-MILC process. The structural characteristics of the implanted by Boron and subsequently crystallized by MILC a-Si films are studied by Transmission Electron Microscopy (TEM) and they are compared to intrinsic a-Si films which were deposited on top, as well as beside the boron implanted a-Si film. During the annealing, spontaneous nucleation occurs in the B-doped films far from the a-c interface, revealing a shorter incubation period in the B-doped films.

Selection and peer-review under responsibility of the Conference Committee Members of NANOTEXNOLOGY2015
(12th International Conference on Nanosciences & Nanotechnologies & 8th International Symposium on Flexible Organic Electronics)

Keywords: Metal Induced Lateral Crystallization, Boron implantation

* Corresponding author. Tel.: ++30-2310-998196; fax: ++30-2310-998929
E-mail address: nikosv@auth.gr

2214-7853
Selection and peer-review under responsibility of the Conference Committee Members of NANOTEXNOLOGY2015 (12th International Conference on Nanosciences & Nanotechnologies & 8th International Symposium on Flexible Organic Electronics)
doi:10.1016/j.matpr.2016.02.015

1. Introduction

Nickel metal induced lateral crystallization of amorphous-Si reduces the crystallization temperature and time, forming very large grains in the order of 10μm. Therefore this process could in the future replace the conventional Solid Phase Crystallization (SPC) in technological applications like Active Matrix Liquid Crystal Displays (AMLCD) [1], active matrix organic light emitting diodes [2] and Large Scale Integrated (LSI) circuits by the realization of single grain devices [3].

The Ni-MILC process is based on the formation of nickel disilicide ($NiSi_2$) precipitates and their one-dimensional migration [4]. The driving force for this movement is the lower chemical potential of Ni at the $NiSi_2$/a-Si interface compared to that of the Ni at the $NiSi_2$/crystalline-Si interface. The disilicide precipitates have the form of regular octahedral, bounded by eight {111} faces having 0.4% lattice mismatch with Si, as schematically shown in Fig1a. The Ni from the leading Si edge of the needle-like crystallite moves to a new leading edge, forming there a new nickel disilicide precipitate to maintain the needle-like crystalline growth along one of the equivalent <111> directions, as schematically shown in Fig.1b, 1c and 1d [4,5].

It was shown that B-implantation in a-Si enhances the crystallization rate during the Ni-MILC process [6,7]. However the structural characteristics and the mode of crystallization were not studied. In the present work the enhanced Ni-MILC is studied after B-implantation by Transmission Electron Microscopy (TEM) and their structural characteristics are revealed.

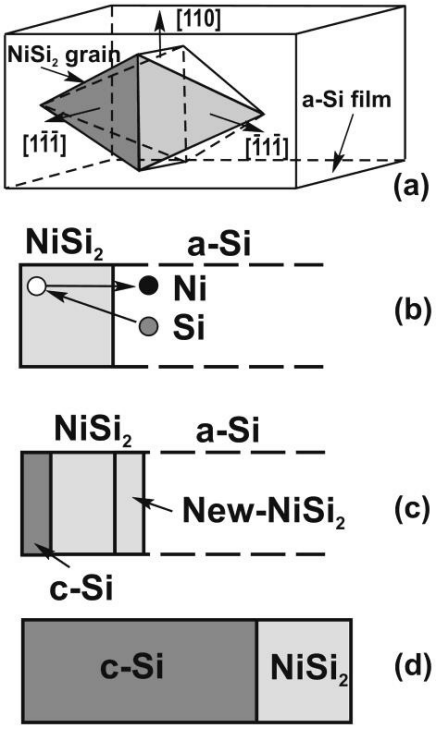

Fig.1 Formation of the Si whisker by the Ni-MILC process: a) The mo——st favorable case is when the [110] direction of the octahedral $NiSi_2$ grains is perpendicular to the a-Si film, because two <111> equivalent directions are parallel to the a-Si film, as schematically shown. b) Ni diffusion from the $NiSi_2$ tip into a-Si. c) Formation of a new $NiSi_2$ layer in front of the whisker and a new crystalline Si layer at the back side of the $NiSi_2$ tip. d) Final whisker

2. Experimental procedure

In order to compare the influence of the B-implantation during the Ni-MILC process in respect of the non implanted a-Si the following configuration shown schematically in Fig.2 was realized by lithography. The substrate was a 3 inch (001) Si wafer which was thermally oxidized so that a 200nm thick SiO_2 buffer layer was formed. On top of this, a 50nm thick intrinsic a-Si layer was deposited by Low Pressure Chemical Vapor Deposition (LPCVD) at 500^{o}C using silane. Subsequently, the intrinsic a-Si film was etched by lithography, so that squared pads with a side of 20 μm were formed. They are denoted by the letter A in Fig.2. The pads were implanted by boron with a dose of $3x10^{13}$ atoms/cm^2 through a protective layer. Then, the protective layer was removed and a second 50nm thick intrinsic a-Si layer was deposited, denoted by the letter B in Fig.2. Therefore, in the area A of Fig. 2 the implanted and the intrinsic a-Si film overlap with the total thickness there to be 100 nm and in area B the thickness is 50 nm. In the next step a 50 nm thick silicon oxide capping layer was deposited by Plasma Enhanced Chemical Vapor Deposition (PECVD). For the Ni-MILC process, long rectangular windows, in the form of strips were opened by lithography on the upper oxide protection layer. Subsequently a 15 nm thick nickel film was deposited on top by vacuum evaporation, so that Ni pads were formed. After that the wafer was annealed at 250^{o}C for 10 minutes in order to form $NiSi_2$. The remnant of the nickel layer was washed off by nitric acid; in this way $NiSi_2$ strips pads were formed, denoted by the letter C in Fig.2a. The wafer was subsequently annealed in nitrogen atmosphere at 590^{o}C for 30min in order to perform the Ni-MILC process. The structural characteristics of the annealed specimens were studied by Plane View TEM (PVTEM) observations. Specimens for PVTEM observations were prepared by etching the upper-level protection SiO_2 layer and the SiO_2 buffer layer using HF and subsequently lifting off the crystallized Si film using gold grids.

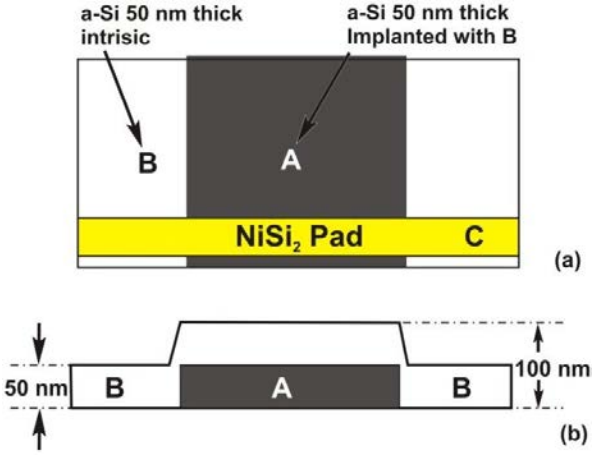

Fig.2 Schematic representation of the two layers of amorphous-Si pads in order to reveal the enhanced Ni-MILC due to Boron implantation: a) In plane view. b) In cross-section. The thickness of the implanted by Boron (dose $3x10^{13}$ atoms/cm^2) film A and of the intrinsic film B was 50nm. The strip C is a 15nm thick Ni film. The specimen at first was annealed at 250^{o}C for 20 min in order to form $NiSi_2$ in the layer C and then it was annealed at 590^{o}C for 30min.

3. Experimental results

As we have seen in Fig.2 the thickness of the a-Si film is 100 nm and 50 nm in areas A and B respectively. However from the literature it is known that the crystallization rate in the Ni-MILC process increases with the thickness of the film [7]. Taking into consideration this parameter we made the following experiment. Some of the pads in the area A in Fig.2 were not implanted, otherwise the specimen was treated as the implanted one. The result is shown in the Plane View TEM (PVTEM) micrograph in Fig.3a.

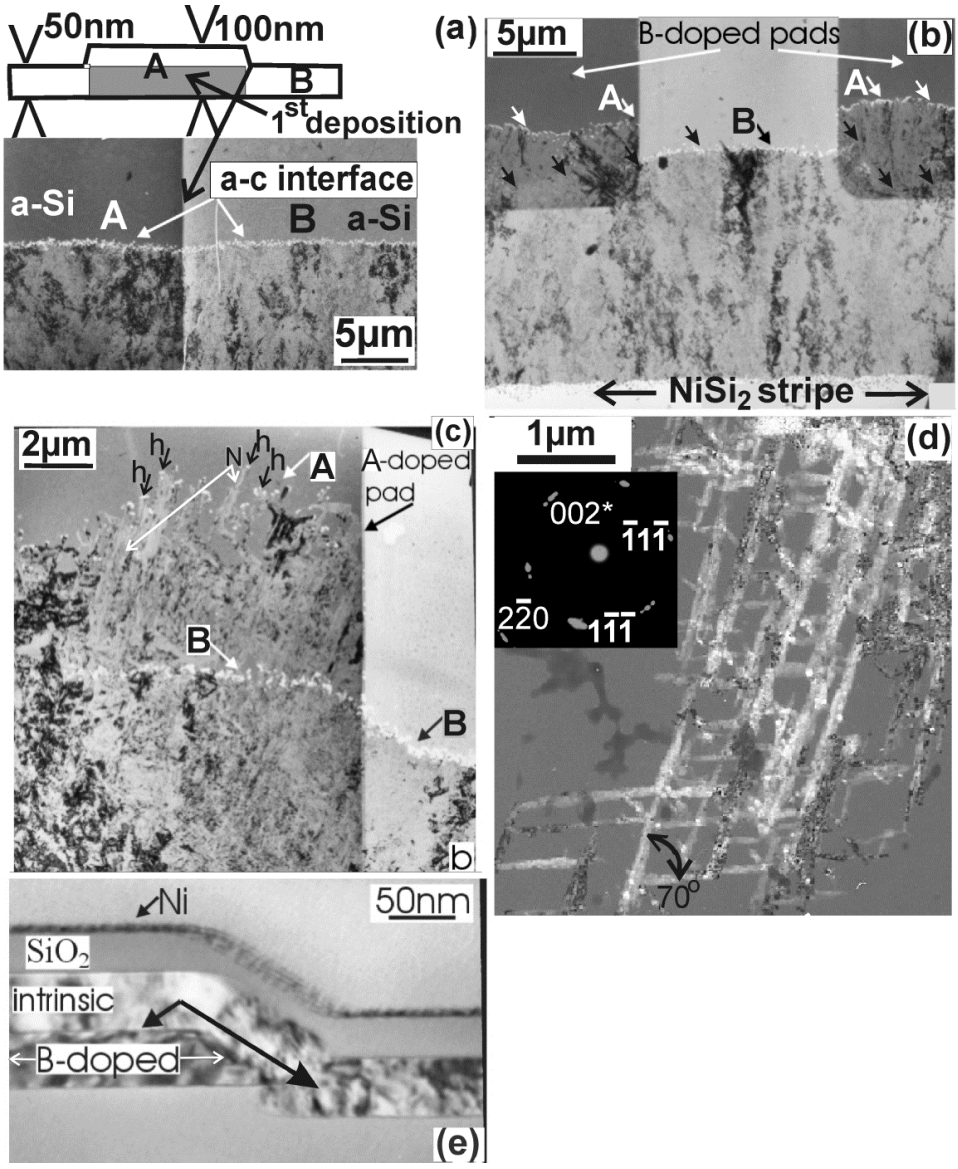

Fig.3 a) Plane view TEM (PVTEM) micrographs of the configuration described in Fig.2. b) In the implanted by Boron areas, denoted by the letter A, two different fronts can be distinguished, denoted by the white and black arrows, respectively. In the contrary only one front exists in the area B. c) The crystallization fronts in the implanted by Boron and the intrinsic a-Si film are clearly shown in the higher magnification PVTEM micrograph. In the implanted film long needle-like crystallites were formed, which advance deep inside the a-Si as shown by the white arrow in area A. d) The whiskers are shown at higher magnification. Two sets of whiskers are observed forming roughly an angle of 70°, very close to the angle between the two {111} equivalent lattice planes. This is confirmed by the selected area electron diffraction (SAED) pattern shown in the inset of figure. This diffraction pattern corresponds to the (110) section with slightly misoriented spots. The two sets of the whiskers coincide to the [1-1-1] and [-11-1] directions. e) Cross-section TEM micrograph taken from the edge of the two overlapping A and B films.

In both areas A and B the amorphous-crystalline (a-c) front is the same, revealing that the crystallization rate is not affected by the thickness of the film at least in this small thickness differences. It is worth noticing that the small white dots observed at the a-c interface are holes attributed to the leading $NiSi_2$ precipitates that were subsequently etched out by the HF solution during the TEM sample preparation. In the implanted by boron areas A two fronts can be distinguished, as shown in Fig.3b, denoted by the white and black arrows respectively. In contrast only one front

exists in the area B. In area A the white arrows correspond to the leading a/c interface of the implanted film. In the same area the black arrows correspond to the retarding intrinsic a-Si film. The crystallization fronts in the intrinsic and the Boron implanted films are also shown in the higher magnification PVTEM micrograph in Fig.3c. Significant differences are observed in the mode of growth of the two films. In the implanted film, long needle-like crystallites were formed advancing deep inside the a-Si as shown by the white arrows in area A. At the tip of each of these whiskers a small hole was formed, denoted by the letter h in Fig.3c which corresponds to the leading $NiSi_2$ precipitate. These whiskers are shown at even higher magnification in Fig.3d. Two sets of whiskers are clearly distinguished forming roughly an angle of 70^o, which is very close to the angle between the two {111} equivalent lattice planes. This is confirmed by the Selected Area Electron Diffraction (SAED) pattern shown in the inset of Fig.3d. This diffraction corresponds to the (110) section with slightly misoriented spots. The two sets of the whiskers coincide to the [1-1-1] and [-11-1] directions in the (110) section. The edge of the pad is shown in the cross-section TEM micrograph in Fig.3e. Some Ni droplets on the capping oxide layer are observed. The interface between the intrinsic and the B-doped silicon layers is clearly delineated.

Boron implantation in a-Si significantly shortens the incubation period increasing also the crystallization rate independently of the MILC process. It has been earlier shown that implantation of doping impurities increases the growth rate, whereas the implantation of non-doping impurities decreases the growth rate, as it was extensively discussed by Licoppe and Nissim [8]. This behavior is attributed to the band bending and related electric field at the amorphous-crystalline interface, with the electric field acting on crystallization through the enhancement of defect migration at the interface [8]. Intrinsic a-Si films annealed at 600^oC require an incubation period of 10 hours for random nucleation. After B-implantation this period is significantly shortened. This is evident in Fig.3 where after a 30 minutes annealing at 590^oC no crystallites were formed in the a-Si due to random nucleation. However, in the same film, a 5 hours annealing at 590^oC results in significant random nucleation inside the a-Si as shown in the PVTEM micrograph in Fig.4. The random nucleation will be an obstacle for the advancing a-c front due to the MILC process, it is evident that random nucleation inhibits the Ni-MILC process reducing the size of the grains. In Fig.4 crystallites up to 1.5 μm in size were formed by random nucleation, as shown by arrows. Some of them are well inside the film which was crystallized by MILC revealing that they were formed before the advancing MILC a-c front.

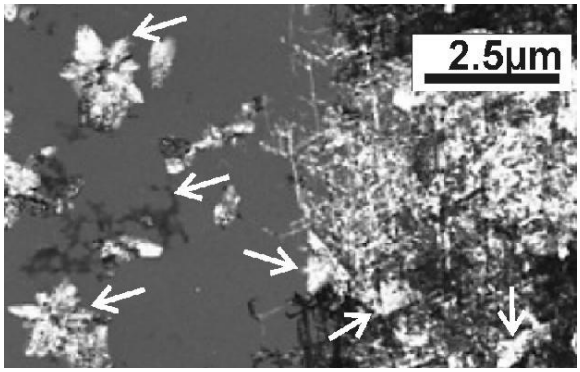

Fig.4 PVTEM micrograph from the Boron implanted pad annealed at 590^oC for 5 hours, spontaneous nucleated in the non crystallized part of the a-Si is evident, denoted by arrows.

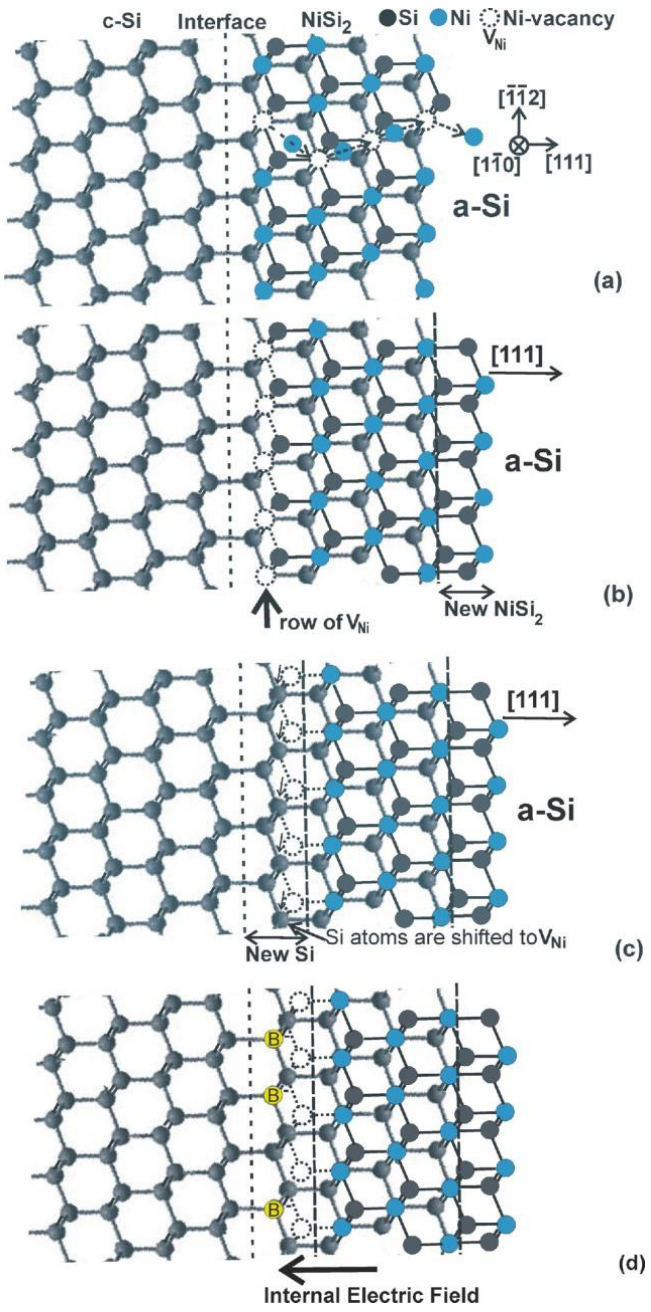

Fig.5 Atomistic representation of the Ni-MILC process and the role of the implanted Boron in a Si whisker with the leading $NiSi_2$ precipitate: a) Ni atoms denoted by blue, are diffused from the leading $NiSi_2$ side into intrinsic a-Si leaving behind Ni vacancies denoted by V_{Ni}. b) A new $NiSi_2$ layer is formed at the front side of the $NiSi_2$ leading edge. The positively charged Ni vacancies V_{Ni} moved towards the c-Si/$NiSi_2$ interface forming there a layer of Ni vacancies. c) By the rearrangement of the bonds of the V_{Ni} a new layer of crystalline Si is formed. Only half of the Si bond must be reformed for the formation of c-Si there. d) Negatively charged Boron ions exist in the depletion region at the Si side in the c-Si/$NiSi_2$ heterojunction after B implantation. Due to electric field in the heterojunction stronger repulsing and attractive forces are induced to the Ni^- ions and the positive V_{Ni} respectively, enhancing the MILC process.

The enhanced MILC process after B-implantation is attributed to a mechanism utilizing the so-called "Ni ion Ni vacancy hopping model" [6]. This is based on the Schottky contact which is formed at the c-Si /$NiSi_2$ coherent interface, as it was proposed by Cherns et. al. [9]. The Ni atoms in $NiSi_2$ phase are negatively charged because of the negative Mulliken charge [10] and act as acceptors in c-Si matrix [6]. For understanding this mechanism at first we studied the Ni-MILC process in the intrinsic a-Si considering a silicon whisker and the related $NiSi_2$ precipitate at the head of it, as shown in Fig.5a. The $NiSi_2$ has the calcium fluoride CaF_2 structure and the Ni atoms, denoted by blue, are diffused from the leading $NiSi_2$ side into intrinsic a-Si leaving behind Ni vacancies denoted by V_{Ni}. Thus a new $NiSi_2$ layer is formed there. The positively charged Ni vacancies V_{Ni} moved towards the c-Si / $NiSi_2$ interface forming there a layer of Ni vacancies, as shown in Fig.5b. By the rearrangement of the bonds of the V_{Ni} a new layer of crystalline Si is formed, as shown in Fig.5c. Only half of the Si bonds must be formed again for the formation of c-Si, which explains the easy Si crystallization by the MILC process.

After B-implantation in a-Si this impurity is not activated unless the doping concentration is higher than the point defect density, which in a-Si is of the order 10^{20} cm^{-3}. In contrast, boron is easily activated in the c-Si, due to the lower defect density there. Consequently, negatively charged boron ions exist in the depletion region at the Si side in the c-Si/$NiSi_2$ heterojunction, as shown in Fig.5d. Therefore stronger repulsing and attractive forces are induced to the Ni- ions and the positive V_{Ni}, respectively by the ionized boron impurities in c-Si/$NiSi_2$ heterojunction enhancing the crystallization rate. The validity of this model was confirmed by phosphorous implantation [6]. In this case retardation of the Ni-MILC process is observed. This behavior is readily explained because the P atoms are positively ionized in the c-Si reversing the electric field in the Schottky contact; consequently retarding the MILC rate. It was also shown that by applying an external electric field the MILC crystallization rate is enhanced in the anode direction, while it is retarded in the cathode direction [11, 12]. This behavior is attributed to the negatively charged Ni-ions in $NiSi_2$ precursor precipitates.

4. Conclusions

The TEM study has shown that Ni-MILC rate was substantially enhanced after B implantation of the a-Si. The crystallization occurs by a bi-directional needle network structure, along to equivalent <111> directions, both perpendicular to [110] direction, as shown in Fig.3d. In the Boron implanted a-Si films spontaneous nucleation is observed revealing a shorter incubation period, which disturbs the MILC process.

Acknowledgements

This research was financially supported in the frame of a Hungarian-Greek bilateral scientific collaboration (project codes TET-10-1-2011-0570 for Hungary and HUN92 for Greece). The European Union under the Seventh Framework Program under a contract for an Integrated Infrastructure Initiative, reference 312483 - ESTEEM2.

References

[1] J. S. Im and R.S. Sposili, MRS Bulletin 21(1996) 39.
[2] S.J. Bae, H.S. Lee, L.Y. Lee, J.Y. Park, C.W. Han, 20th Int. Display Research Conference 2000, Palm Beach, USA, 2000, pp. 358.
[3] K. Makihira and T. Asano, Int. Workshop on Active-Matrix Liquid-Crystal Displays (2000 Tokyo), pp. 33.
[4] C. Hayzelden and J. L. Batstone, J. Appl. Phys. 73 (1993) 8279.
[5] J. Jang, S. J. Park, K. H. Kim, B. R. Cho, W. K. Kwak and S. Y. Yoon, J. App. Phys. 88 (2000) 3099.
[6] Ji-Su Ahn, Yeo-Geon Yoon, Seung-Ki Joo, J. Crys. Growth 290 (2006) 379.
[7] T. Ma and M. Wong, J. Appl. Phys. 91 (2002) 1236.
[8] C. Licoppe and Y. I. Nissim J. App. Phys. 59 (1986) 432.
[9] D. Cherns, G. R. Anstis, J. L. Hutchison and J. C. H. Spence, Phil. Mag. A, 46:5 (1982) 849.
[10] J. Jang, J.Y. Oh, S.K. Kim, Y.J. Choi, S.Y. Yoon, C.O. Kim, Nature 395 (1998) 481.
[11] C.H. Yu, P.H. Yeh, L.J. Chen, Nuclear Instruments and Methods in Physics Research B 237 (2005) 167–173
[12] Ji-Su Ahn, Deok-Kee, Kim and Seung-Ki Joo, J. Appl. Phys. 113 (2013) 223509.